ELSEVIER

Microporous and Mesoporous Materials 52 (2002) 105–117

MICROPOROUS AND MESOPOROUS MATERIALS

www.elsevier.com/locate/micromeso

Porosity development in activated carbons obtained from date pits under chemical activation with phosphoric acid

Badie S. Girgis*, Abdel-Nasser A. El-Hendawy

National Research Centre, Laboratory of Surface Chemistry, 12622 Dokki, Cairo, Egypt

Received 5 February 2001; received in revised form 15 November 2001; accepted 27 November 2001

Abstract

Date pits, a low-cost agricultural by-product, was tested as a precursor for the production of porous carbons in a chemical scheme using phosphoric acid. The raw material was impregnated with increasing concentrations of H_3PO_4 (30–70 vol.%) followed by pyrolysis at 300, 500 or 700 °C. Texture characteristics of the products were determined by adsorption of N_2 at 77 K, as well as iodine, phenol, and methylene blue values. Carbons obtained at 300 °C were very poorly porous, although with anomalously high capacity for the uptake of probe molecules from solution. This was attributed to the contribution of unsaturated chemical bonds initiated in the partially decomposed material. Carbons obtained at 500 and 700 °C are good to excellent adsorbents and attain best developed porosity at 700 °C, contrary to the earlier well-established temperature of 500 °C recommended for treatment of agricultural precursors. Thermogravimetric/differential thermogravimetric tracings of the H_3PO_4-impregnated date pits indicated a delayed-decomposition effect shifted to higher temperature as compared to the raw material. Phosphoric acid is suggested to inflict physical and chemical modifications on the botanical structure by penetration, particle swelling, partial dissolution of the biomass, bond cleavage and reformation of new polymeric structures resistant to thermal decomposition. In addition, raw date pits are proposed to be composed of a low-porosity and compact cellular structure that needs higher acid concentrations and/or temperatures to attain the optimum effect normally reached at lower temperature in case of other feedstocks of botanical origin.

Keywords: Porosity; Activated carbon; Date pits

1. Introduction

Activated carbon (AC) is perhaps one of the most widely used adsorbents. Over the last few decades, adsorption systems involving AC has gained importance in purification and separation processes on an industrial scale. It is now considered as one of the best available technologies in removing both organic and inorganic trace contaminants. Its use can be broken down into discrete areas such as effluent treatment, potable water treatment, solvent recovery, air treatment, decolorizing, metal ore processing, and many more general domestic applications. This explains the increasing market trend for the use of ACs [1]. They owe their distinguished properties to the extensive surface area and internal porosity, as well as their developed surface structure. The inherent nature of the precursor, or starting material, as

* Corresponding author.

1387-1811/02/$ - see front matter
PII: S1387-1811(01)00481-4

well as the methods and conditions employed for carbon synthesis, determine the final pore size distribution and the adsorption properties of the AC [2,3].

ACs can be produced from virtually any carbonaceous precursor, both naturally occurring and synthetic. Process economics normally dictate the selection of readily available, low-cost feedstocks. Common examples of commercial carbon feedstocks are materials of botanical origin (e.g. wood, coconut shells, and fruit stones) and degraded or coalified plant matter (e.g. peat, lignite and all ranks of coal). A list of the most common raw materials, as given by Bansal et al. [4], reads as follows: wood, 35%, coal, 28%, lignite, 14%, coconut shells, 10%, peat, 10% and others, 3%. Precursors from fresh biomass origin offer the most economical source because they are copious renewable supplies, with low mineral content and appreciable hardness, and of low cost. The literature pertaining to the use of agricultural by-products (lignocellulosics) is very extensive, however, coconut shells are still receiving renewed attention [5,6], next we meet: almond shells, peach stones, apricot stones, plum stones, cherry stones and nutshells (such as hazelnuts, walnuts, cashew and macadamia nuts) [7–17]. In comparison, date pits received much less consideration as a source material for the preparation of AC [18–21].

The methods of activation commonly employed can broadly be divided into two main types: thermal (or physical) activation and chemical activation. Thermal activation involves primary carbonization (below 700 °C) followed by controlled gasification under the action of oxidizing gases at high temperature (up to 1100 °C) [4]. In chemical activation the precursor is mixed with a chemical restricting the formation of tars (e.g. $ZnCl_2$, H_3PO_4, etc.), after kneading carbonized and washed to produce the final AC. The chemical incorporated into the interior of the precursor particles reacts with the thermal decomposition products reducing the evolution of volatiles and inhibits the shrinkage of the particles. In this way, the conversion of the precursor to carbon is high, and once the chemical is eliminated after the heat treatment, a large internal porosity is formed [22]. Phosphoric acid activation only involves a single heat treatment step and is achieved at lower temperatures (400–500 °C), higher yields are obtained and most of the phosphoric acid can be recovered after the process is completed. Thus, it is a material-, energy- and time-saving scheme for the production of ACs. Its use as an activating agent is now more favored over $ZnCl_2$, not only because of the simplicity of the extraction process after carbonization and impregnant recovery (only water is required), but also on account of the decline of the $ZnCl_2$ process due to problems of environmental contamination with zinc compounds [23].

In earlier investigations, we dealt with activation using H_3PO_4 for the production of good adsorbing carbons derived from various agricultural by-products (sugar cane bagases [24], apricot stone shells [25], rice hulls [26], corn cobs [27,28], cotton stalks [29], olive mill wastes [30], and peanut hulls [31]). Date pits represent an equally abundant by-product generated from food processing and jam production industries. In Egypt, date palms exceed eight million trees which generate a considerable amount of low-cost, non-valuable waste material. Our previous experience with the above-mentioned plant wastes urged the present investigation, as date pits are hard, high-density low-ash fruit kernels. These qualities recommend them for the production of granular ACs suitable for fixed-bed purification systems, as well as in regeneration schemes. In earlier studies date pits were essentially subjected to thermal activation in two-step [18–21] or in one-step steam pyrolysis [32] procedures, which urged their treatment in the well-established chemical activation with H_3PO_4.

The present study describes the preparation and porosity evaluation of ACs from date pits at increasing concentrations of H_3PO_4 and/or heat treatment temperatures (HTTs). It aims at demonstrating the potential of utilizing this precursor, and the development of its porosity as a function of varying conditions of treatment, by analysis of the N_2 adsorption isotherms at 77 K applying various procedures. Additional information is obtained from adsorption experiments of various probe molecules from aqueous solution. Description of the impact of the activation process on porosity development is displayed, based on cur-

rent literature, and in light of the texture parameters obtained. This contribution is intended to complement previous studies in a program dedicated to the development of ACs from locally available low-cost agricultural by-products. Such a process would serve a double purpose. First, it converts undesirable, surplus agricultural waste, of which millions of tons are produced annually, to useful value-added adsorbents. Second, the produced ACs find increasing applications in water treatment, and other fields. This would contribute to solving many current-day environmental pollution problems.

2. Materials and methods

2.1. Activated carbons

Washed-clean whole date pits were dried in an air oven at 80 °C for 48 h, which proved effective to facilitate subsequent crushing and grinding. Sixty grams of the crushed pits (0.5–2.0 mm in size) were mixed with 100 cm^3 of prediluted H_3PO_4 (85 wt.%) to varying concentrations in the range 30–70 vol.%. The slurry was left overnight at room temperature, then transferred to a stainless steel reactor (diameter of 40 mm and length of 60 cm) with narrow ports of 10 mm diameter at both ends. Exhaust gases and liquid condensates are vented through these openings. The reactor is admitted into an electric tube furnace and heated at a slow rate ($\sim$5 K min^{-1}), to allow free evolution of volatiles, up to the hold temperatures 300, 500, or 700 °C. Soaking at each final temperature was conducted for 2 h. The cooled mass was subjected to thorough washing with hot water until the washings were neutral in effect, then dried at 110 °C for 24 h, and finally kept in tightly closed bottles. Carbon yield ranged from 38% to 43%. Fifteen samples were thus obtained and given notations including two numerals; the first denotes the HTT (3 = 300°, 5 = 500° and 7 = 700 °C) and the second number indicates the acid concentration (3–7 denotes 30–70 vol.%). A carbon sample 55, thus, represents the product obtained by heat treating the precursor at 500 °C and preimpregnated with 50 vol.% H_3PO_4.

2.2. Characterization of the porosity

This was carried out by determining the adsorption isotherms of N_2 at 77 K by the help of a vacuum apparatus of the conventional type. Some adsorption data were obtained by an automatic recording apparatus of the type ASAP 2010 (a product of Micromeritics, Inc.) which showed essentially similar results. The tested carbons were out-gassed under vacuum at 200 °C for 2 h prior to starting the measurements. Adsorption data were analyzed by applying the BET equation, the α_s-method [33] and the DR-plot [34]. Thus, the adsorption data (V_a, $cm^3\,g^{-1}$) were plotted against the α_s-values reported by Selles-Perez and Martin-Martinez [35] for the N_2 adsorption on a non-porous carbon material. The linear section connecting to the origin corresponds to the specific surface area (S_t^{α}), and the linear relation at and beyond $\alpha_s \geqslant 1.0$ describes the non-microporous surface area (S_n^{α}) whereas its intercept with the V_a-axis gives the micropore volume (V_0^{α}). Plots for the DR equation are in the form $\ln n_a$ (n_a, mmol g^{-1}) vs. $[A/\beta]^2$, where $A = \mathrm{RT}\ln P^0/P$ and $\beta = 0.35$, such that the intercept of the rectilinear relationship measures the micropore volume (V_0^{DR} mmol g^{-1}) and the slope equals $(1/E^0)^2$ [36].

In addition, the mesopore volume (V_{meso}) was obtained from the volume of nitrogen, as liquid, adsorbed for each sample between $P/P^0 = 0.1$ and 0.95, as suggested earlier [37].

2.3. Adsorption from solution

The iodine and phenol numbers were determined by using the single bottle point uptake from 0.02 M iodine solution, or 100 mg l^{-1} solution of phenol, respectively. Adsorption isotherms for methylene blue (MB), from aqueous solution, were determined by contacting fixed amounts of the predried powdered carbon sample (200 mg) with 100 cm^3 of the dye solution of varying initial concentrations. The stoppered bottles were agitated for 24 h, at room temperature, and the filtered solution was measured for the residual color at $\lambda = 664$ nm by the help of a UV/VIS recording spectrophotometer produced by Shimadzu (2401 PC).

2.4. Thermogravimetric analysis of date pits

In order to detect the effect of phosphoric acid on the raw material thermogravimetric (TG) and differential thermogravimetric (DTG) recordings were determined. The raw finely powdered date pits and a sample impregnated with 50 vol.% H_3PO_4 (dried at 105 °C) were analyzed. An apparatus of the type Perkin–Elmer 7 Series Thermal Analysis system was used at a heating rate of 10 K min^{-1} up to 900 °C.

3. Results

3.1. Modifications in the course of pyrolysis under the action of phosphoric acid

During the pyrolysis of lignocellulosic materials, three stages can be distinguished [22]. These are: (a) loss of water in the 300–573 K range, (b) primary pyrolysis in the 573–773 K range with evolution of most gases and tars with formation of the basic structure of the char, and (c) consolidation of the char structure at 773–1123 K with a small weight loss. Despite the influence of the intrinsic chemical composition (relative content of the constituents: cellulose, hemicellulose and lignin), the extrinsic factor of the chemical impregnant would be equally effective in directing the course of pyrolysis.

According to Fig. 1, raw date pits (DP) exhibit only one prominent wave of weight loss (between 200 and 400 °C) with a maximum centered at 270 °C, followed by a slow weight loss with decreasing rate. A considerably different pattern is exhibited by the H_3PO_4-treated lignocellulosic material (DPP). A regular small weight loss covers the early stage between ambient and 400 °C, with a broad weak peak around 250 °C, followed by another slow higher weight loss with increasing temperature from 400 to 700 °C. Beyond this temperature the decomposing mass is still showing loss in weight at a slower rate up to 900 °C. Through this temperature range of 400–900 °C two DTG peaks appear with maxima at 525 and 700 °C.

Thus, impregnation with H_3PO_4 brings about considerable effects on the course of pyrolysis of

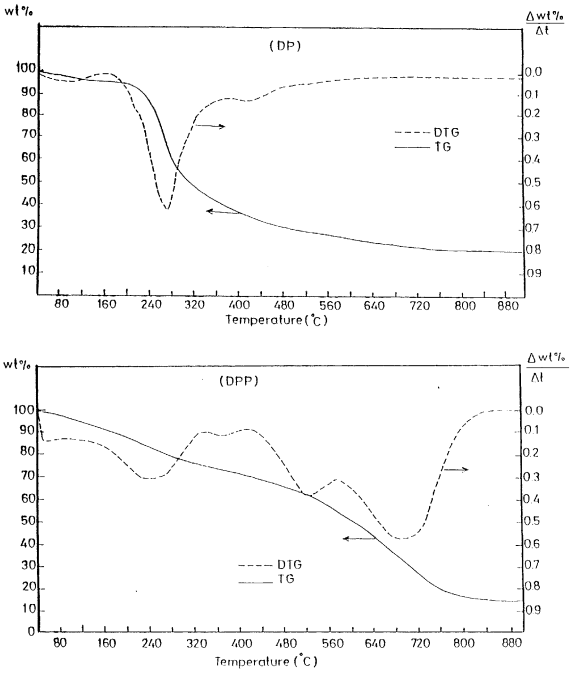

Fig. 1. TG and DTG for date pits (DP) and H_3PO_4-impregnated date pits (DPP).

date pits (see Fig. 1 and Table 1): (i) it shifts degradation to considerably higher temperatures, (ii) it enhances the early dehydration stage combined with an evolution of low-boiling volatiles (cf. 12% and 5%, respectively), (iii) it strongly retards the evolution of volatiles, where up to 600 °C only around 50% weight is lost, whereas in the absence of H_3PO_4 complete degradation is finished before

Table 1
Weight loss of date pits (DP) and H_3PO_4-impregnated date pits (DPP) within different ranges of temperatures

Temperature range	Δ wt.%	
	DP	DPP
r.t.–200	4.9	11.9
200–300	41.5	10.9
300–400	17.0	5.6
400–500	7.1	6.0
500–600	4.5	14.2
600–700	2.7	29.1
700–800	1.8	14.8
r.t.–800	79.5	83.5

r.t. = Room temperature.

450 °C, (iv) it effectively suppresses the principal degradation stage (200–400 °C) as it is accompanied by a weight loss of only 17% in presence and 58% in the absence of H_3PO_4, and (v) it promotes the carbon yield within the range of 400–700 °C. These observations could be reasonably associated with the suggested mechanism, involving dissolution of some chemical components with bond cleavage, followed by recombination at other sites forming new polymeric structures that are thermally more resistant [38].

3.2. Variations in porosity characteristics as a function of the conditions of preparation

3.2.1. General features of the N_2 adsorption isotherms

Figs. 2–4 give illustrative examples for the shape and behavior of the N_2 adsorption isotherms, and of the α_s- and DR-plots, for the series of carbons obtained at 300–700 °C at varying H_3PO_4 concentrations. The isotherms (Fig. 2) approach the Type I (Langmuir) with small upward bending at higher pressure, indicating an essentially microporous character with some contribution of wider pores (meso- and macropores), as will be demonstrated by the evaluated parameters. The α_s-plots (Fig. 3) show two linear sections: one connecting the early points up to $\alpha_s \approx 0.8$ and another one connecting the high-pressure data with a considerable slope corresponding to the non-microporous surface area (type α-1b, [39]). In many cases it was not possible to join the origin

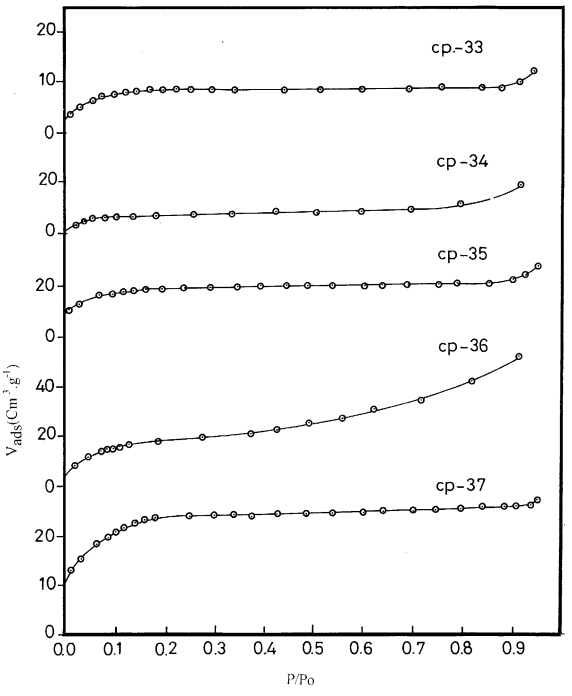

Fig. 2. Representative adsorption isotherms of N_2 at 77 K on ACs obtained at 300 ° C.

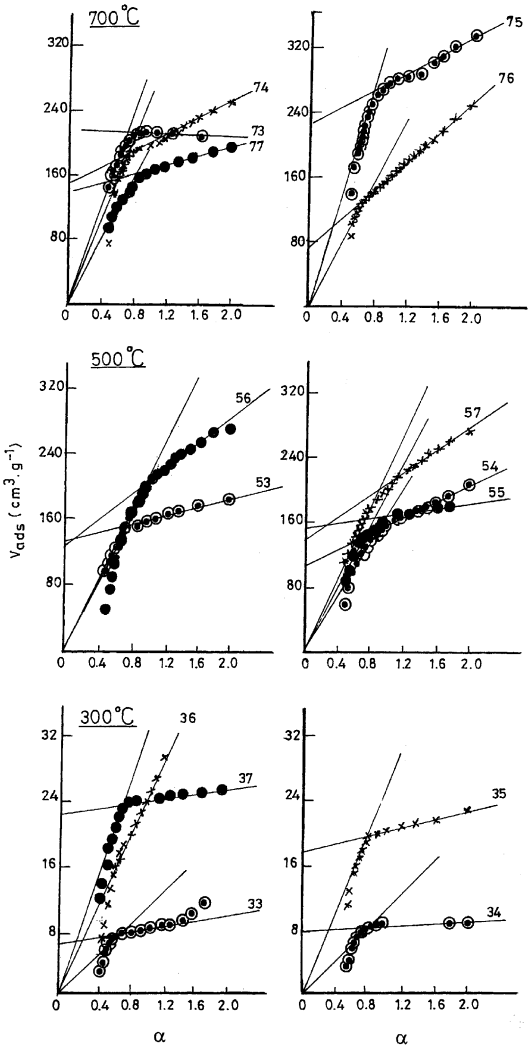

Fig. 3. α_s-Plots of N_2/77 K isotherms for ACs obtained at 300–700 °C.

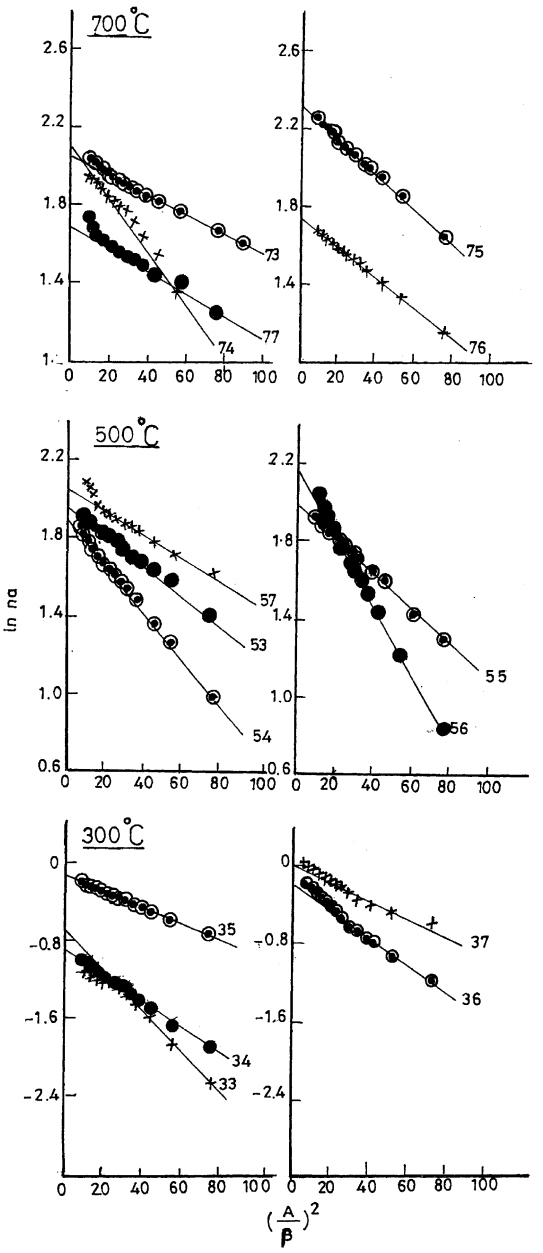

Fig. 4. DR-linear plots for the N_2/77 K isotherms for ACs.

with the points located at the lower α_s-values, and a negative deviation appears. This kind of deviation was described as due to the presence of a primary and secondary micropore filling mechanism [39].

On the other hand, the DR-plots (Fig. 4) indicate a type C behavior, with a small upward bending at high pressures (low $(A/\beta)^2$ values) which results from adsorption in pores wider than those associated with micropore filling and are therefore a consequence of a bimodal distribution of A with V [36]. However, the estimated micropore volumes (V_0^{DR}) are mostly higher than the V_0^{α} values (Tables 2–4), which is generally attributed to an overlap between adsorption in narrow and wide micropores [37]. This also leads to higher estimates of S^{KDR} as compared to S_t^{α} values, whereas the latter values are mostly concordant with the S_{BET} surface areas (Tables 2–4).

It is of interest to compare the P/P^0 values that realize the V_0^{α} and V_0^{DR} estimates which are

Table 2
Texture characteristics of ACs obtained at 300 °C in the presence of varying H_3PO_4 concentrations

Parameter	30%	40%	50%	60%	70%
	C33	C34	C35	C36	C37
S_{BET} ($m^2\,g^{-1}$)	28	33	68	71	86
V_p ($cm^3\,g^{-1}$)	0.034	0.017	0.056	0.082	0.040
V_{meso} ($cm^3\,g^{-1}$)	0.024	0.005	0.013	0.057	0.009
S_t^{α} ($m^2\,g^{-1}$)	28	28	72	68	79
S_n^{α} ($m^2\,g^{-1}$)	12	5	6	–	5
S_{mic}	16	23	66	68	–
V_0^{α} ($cm^3\,g^{-1}$)	0.005	0.011	0.028	–	0.033
V_0^{DR} ($cm^3\,g^{-1}$)	0.017	0.015	0.031	0.030	0.038
E_0 ($kJ\,mol^{-1}$)	7.0	8.5	11.2	8.5	9.5
S^{KDR} ($m^2\,g^{-1}$)	49	42	86	83	106
X_p	0.72	0.96	1.20	1.44	1.68

Table 3
Texture characteristics of ACs obtained at 500 °C in the presence of varying H_3PO_4 concentrations

Parameter	30%	40%	50%	60%	70%
	C53	C54	C55	C56	C57
S_{BET} ($m^2\,g^{-1}$)	546	498	556	647	635
V_p ($cm^3\,g^{-1}$)	0.304	0.321	0.296	0.437	0.459
V_{meso} ($cm^3\,g^{-1}$)	0.030	0.188	0.086	0.222	0.221
S_t^{α} ($m^2\,g^{-1}$)	549	484	547	629	627
S_n^{α} ($m^2\,g^{-1}$)	80	174	83	238	197
S_{mic}	469	370	464	391	430
V_0^{α} ($cm^3\,g^{-1}$)	0.199	0.131	0.227	0.187	0.212
V_0^{DR} ($cm^3\,g^{-1}$)	0.243	0.229	0.248	0.288	0.266
E_0 ($kJ\,mol^{-1}$)	11.4	9.1	10.8	7.6	13.1
S^{KDR} ($m^2\,g^{-1}$)	679	642	695	808	747

Table 4
Texture characteristics of ACs obtained at 700 °C in the presence of varying H_3PO_4 concentrations

Parameter	30%	40%	50%	60%	70%
	C73	C74	C75	C76	C77
S_{BET} ($m^2\,g^{-1}$)	740	733	945	520	522
V_p ($cm^3\,g^{-1}$)	0.372	0.482	0.545	0.415	0.329
V_{meso} ($cm^3\,g^{-1}$)	0.075	0.129	0.187	0.181	0.125
S_t^α ($m^2\,g^{-1}$)	810	695	934	560	554
S_n^α ($m^2\,g^{-1}$)	14	118	155	242	112
S_{mic}	796	477	779	318	442
V_0^α ($cm^3\,g^{-1}$)	0.317	0.258	0.346	0.218	0.191
V_0^{DR} ($cm^3\,g^{-1}$)	0.331	0.336	0.424	0.239	0.229
E_0 ($kJ\,mol^{-1}$)	13.8	8.9	10.6	11.5	13.1
S^{KDR} ($m^2\,g^{-1}$)	928	942	1188	671	643

observed as 0.03–0.14 and 0.18–0.80, respectively, where the latter values are definitely too high and unreasonable. Filling of micropores, as postulated by the theory of volume filling of micropores cannot be believed to continue up to such very high-pressure ranges. This phenomenon ($V_0^{DR} > V_0^\alpha$) has been observed earlier with several ACs obtained by H_3PO_4 activation from various precursors [28,29,40,41]. Such a behavior seems thus particular to the H_3PO_4-activated carbons, whereas in case of steam-activated carbons small differences appear in both surface area and pore volume estimations [32]. This may be associated with the highly developed porosity with a wide range of pore sizes in which pore filling overlaps to result in such a behavior. Another possible view may be proposed which explains the effect and the negative intersection in the early region of the α_s-plots (see above). It seems that, at very low pressures, diffusion of the adsorbed N_2 molecules at 77 K is very slow, due to the presence of constrictions at the entry of the micropores and/or to depositions of the unleached residual phosphates. The low volume of adsorbed nitrogen will deform the initial linear section of the DR relationship by shifting it downwards and consequently leads to high slopes measuring low E_0 values (cf. 7.0–13.8 $kJ\,mol^{-2}$) as well as to the observed high intercepts corresponding to the $\ln V_0^{DR}$ values (Tables 2–4). Probably, much longer times are needed to attain equilibrium conditions at the early adsorption pressures. Restricted diffusion of N_2 at 77 K in chars and ACs has been observed in many cases as mentioned by Carrasco-Marin et al. [42]. In such cases adsorption of CO_2 at temperatures around ambient showed different estimates for the microporosity than the N_2/77 K results. It should be noted that this trend applied to the data from the conventional vacuum system as well as the automated ASAP unit. An equilibrium duration of 10–15 min in the early isotherm region seems to be insufficient to satisfy the activated diffusion of nitrogen into the micropores.

Mixed micro-mesopore adsorbents are thus apparent, although the contribution of mesoporosity is lower in comparison to the microporosity (cf. S_n^α and S_t^α, Tables 2–4). This appears more evident by comparing V_0, V_{meso} and V_p, V_0^{DR}, S^{KDR}, as well as the low E_0 values (denoting wide micropores) as well as the average pore widths (13–25 Å).

3.2.2. Influence of heat treatment temperature on the development of porosity

It has been established by several investigators that, in case of H_3PO_4 treatment of agricultural materials, temperatures around 450 °C are most suitable to obtain optimum properties of the ACs [7,24–30,43–47]. Even a temperature of 300 °C was found sufficient, in some cases, to produce active carbons with developed porosity (e.g. apricot stones with S_{BET} of $\sim$1200 $m^2\,g^{-1}$). For the present precursor, date pits, a temperature of 300 °C has no influence on the poorly adsorbing char at this temperature (Table 1). Increased acid concentration, or the acid: precursor ratio (X_p), slightly raises the porosity from 38 to 86 $m^2\,g^{-1}$, which is due to the aggressive action on the cellular structure.

Raising the HTT to 500 °C (the previously established optimum range) has a good influence on the raw material with a generation of moderately developed porosity (S_{BET} = 500–630 $m^2\,g^{-1}$, V_p = 0.30–0.46 $ml\,g^{-1}$). This effect is enhanced with the concentration of H_3PO_4 which indicates the suitability of this temperature for the evolution of porosity. It is astonishing that, at a still higher temperature of 700 °C, development of better adsorbing carbons is attained with a S_{BET} reaching 950 $m^2\,g^{-1}$ with a corresponding total pore volume

of 0.55 ml g^{-1}. With many earlier studies this temperature was mostly associated with an apparent reduction in porosity which was ascribed to the breakdown of the microporous structure resulting in an evolution of wider porosity characterized by lower internal surface area. The present precursor, however, exhibits a generation of porosity essentially in the micropore range at 700 °C.

It may be suggested that the abnormal response of date pits towards activation with H_3PO_4 can be attributed to its special compact botanical structure. The relatively loose cellular structure of several lignocellulosic materials, exhibiting low particle density and high inherent porosity, facilitates better contact and penetration of the impregnant. Such action leads to considerable physical and chemical structural modifications which is accordingly reflected by the properties of the carbons developed at relatively lower temperatures. This specific nature of date pits would explain their inertness at 300 °C, as well as the extended activating action of H_3PO_4 up to 700 °C, rather than up to ≈500 °C . It is worth mentioning that simple carbonization of date pits at 500 and 700 °C produced chars of negligible porosity ($S_{BET} < 20$ $m^2 g^{-1}$, $V_p < 0.01$ $cm^3 g^{-1}$) [32] which demonstrates the important effect of H_3PO_4 in porosity generation.

3.2.3. Influence of the H_3PO_4 concentration on porosity development

To demonstrate the effect of the amount of acid introduced into the particles after impregnant dehydration, the so-called "degree of impregnation" is calculated. It expresses the weight of acid retained per gram of raw precursor and is denoted by X_p [23]. As this ratio is increased it will intensify the action of the acid in two ways: (a) by increasing the aggressive physico-chemical effect on the raw lignocellulosic material and (b) upon dehydration, inside and between the original botanical cellular structure, the acid creates much porosity that is prevented from contraction or collapse. Subsequent leaching by exhaustive washing will evacuate and free this internal porosity and leave behind an extensive porosity.

The impregnation ratios applied ($X_p = 0.72$–1.68) are hardly effective at 300 °C, but more clearly efficient at 500 °C. However, the intensive action in generating porosity at 500 °C is not correspondingly related with the increase of the amount of impregnant. An optimum value of ≈1 $X_p = 1.44$ seems to be sufficient for a maximum effect, which is somewhat higher than that observed before with other precursors [24,25,27,30]. Additional acid is not benificial, as it does not lead to further action and probably forms an insulating layer (or skin), covering the particles, thus reducing the activation process and the contact with the surrounding atmosphere [45].

For carbons obtained at 700 °C, an increased impregnation ratio seems to generate more porosity. An optimum effect of acid occurs at $X_p =$ 1.20 which yields the best adsorbing carbon with $S_{BET} = 945$ $m^2 g^{-1}$ and $V_p = 0.545$ $cm^3 g^{-1}$. Introduction of more acid into the particles degrades the porosity, which might be explained as above: the surplus dehydrated acid forms an insulating layer that limits the action of the activant considerably and reduces the formation of area-responsible micropores as observed in the considerable decay in S_{mic} as well as V_0^{α} values (Table 4).

3.3. Adsorption capacity from aqueous solutions

3.3.1. Iodine and phenol numbers

It has been established that the iodine number (in mg g^{-1}) gives an estimate of the surface area (in $m^2 g^{-1}$) [8], and it measures the porosity for pores with dimensions $\geqslant 1.0$ nm. Here, a difference between the iodine number and S_{BET} is observed for ACs obtained from date pits at and beyond 500 °C (Table 5). A lower adsorption of iodine can be ascribed to the presence of pores narrower than 1.0 nm, which largely makes up most of the structure of these carbons. For carbons pyrolyzed at 500 °C the accessible ratio of surface is generally high (0.85 up to 1.00), whereas carbons produced at 700 °C exhibit a much lower capacity indicating considerable ultra-microporosity (ratio of $S_I/S_N^{\alpha} = 0.47$–0.67). These carbons contain mostly micropores with a small contribution of mesoporosity. This is confirmed by the various texture parameters (Table 4). In particular, sample 76 shows a high S_I/S_N^{α} ratio of 0.85 and contains

Table 5
Iodine and phenol numbers for the tested ACs

Sample notation	pH	Iodine no. (mg/g)	S_I/S_N^{α}	Phenol no. ($mg\,g^{-1}$)	S_{Ph} ($m^2\,g^{-1}$)	S_{Ph}/S_N^{α}
33	6.23	183	(5.9)	59	165	(5.32)
34	6.1	193	(8.0)	75	210	(8.75)
35	5.9	203	(2.9)	64	179	(2.56)
36	5.63	213	(3.4)	44	123	(1.98)
37	5.23	228	(2.7)	64	179	(2.1)
53	5.48	508	0.925	132	370	0.673
54	5.48	518	1.00	146	409	0.807
55	5.23	518	0.921	132	370	0.657
56	5.01	523	0.977	127	355	0.663
57	4.02	528	0.853	118	330	0.553
73	4.71	366	0.472	120	336	0.434
74	4.68	477	0.675	110	308	0.435
75	4.4	508	0.537	166	465	0.492
76	4.18	457	0.856	151	423	0.792
77	4.01	345	0.616	162	453	0.809

considerable mesoporosity (S_n and V_{meso}) with low V_0^{α}.

An anomalous behavior is observed for the 300 °C products with very poor porosity which show a high capacity for iodine. Thus, they take up 183–228 $mg\,g^{-1}$ which correspond to 2.7 up to 8.0 times the N_2-surface areas. These values might suggest a non-adsorptive process, and are probably associated with an addition reaction of iodine to available double bonds in the partially pyrolyzed lignocellulosic material. This process would contribute largely to the consumption of high amounts of iodine, and such a phenomenon was currently observed with other plant precursors (e.g. peanut hulls [31]).

It is worthwhile mentioning that these specific carbon products also exhibit a high capacity for the removal of phenol from aqueous solutions (44–75 $mg\,g^{-1}$) (Table 5). Considering that the area covered by an adsorbed phenol molecule in a flat orientation equals 0.52 nm^2 [48], anomalously high surface areas are evaluated which correspond to degrees of coverage similar to the iodine values (2.0 up to 8.8). Such values cannot be accounted for by simple physical adsorption by the poorly porous adsorbents. It confirms, furthermore, the above observation with regard to the chemical nature of the surface of these carbon adsorbents.

On the other hand, removal of phenol by the ACs obtained at 500 and 700 °C is related to their porosity characteristics which determine the degree of accessibility of these molecules. The degree of coverage for these carbons ranges from 43% to 81%. The determined values are comparable to those for many commercial carbons and appear even higher even than those of some products [49–51].

3.3.2. Adsorption of methylene blue

MB is one of the most widely recognized probe molecules for assessing the removal capacity of a specific carbon for moderate-size pollutant molecules ($\geqslant 1.5$ nm). Fig. 5 illustrates the adsorption isotherms of MB on the carbons under consideration, which are of the type L (Langmuir) tending to a plateau parallel to the C_e-axis. Both the Langmuir and Freundlich equations were applicable and showed satisfactory straight lines through the whole concentration range. Table 6 summarizes the adsorption parameters derived from both adsorption models. Adopting the well-established value of 1.20 nm^2 covered by a flat adsorbed MB molecule [52], the estimated monolayer capacities (q_m) were converted into surface areas accessible to MB (S_{MB}).

Again, the 300 °C carbons seem to adsorb such amounts of MB that appear to measure much higher surface areas. However, this trend may be explained if MB is imagined to be adsorbed in a compact state in micelles with an aggregate

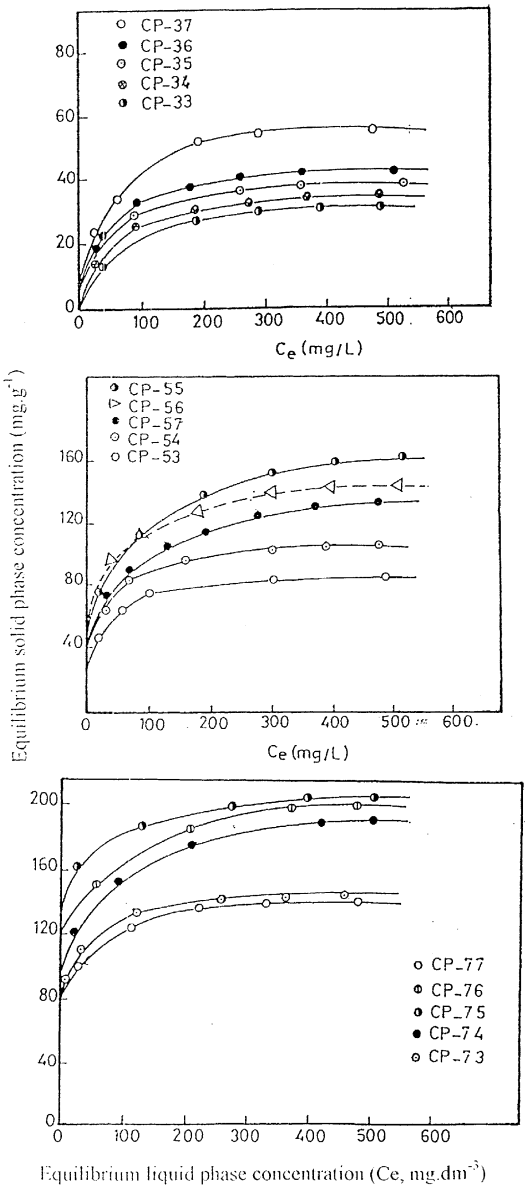

Fig. 5. Adsorption isotherms of MB for the investigated carbons.

number $n = 2$ as suggested earlier by Giles et al. [52]. This brings the area values to within the estimated N_2-surface areas, i.e. 36, 41, 47, 49 and 82 $m^2 g^{-1}$ (cf. Tables 2 and 4), which means a more or less complete coverage of the charred surface with a monolayer of aggregated dye molecules.

For the ACs obtained at 500 or 700 °C, MB is adsorbed in a manner determined by the texture characteristics of each adsorbent. The prevailing microporosity, thus, limits considerably the uptake of MB by most carbons so as to attain values lower than those recommended for adsorbing carbons of 200 mg g^{-1} (cf. most of the present values range between 84 and 160 mg g^{-1}). Only three carbons conform to the required limit. These are samples nos. 74, 75 and 76 obtained at 700 °C. This confirms the above-described observations concerning the high surface area and developed porosity particularly within the wide micro- and mesopore range. The effective factor is the impregnant concentration which lies within 50% and 60% H_3PO_4 (corresponding to a degree of impregnation equivalent to 1.20–1.44).

4. Discussion

The action of phosphoric acid in the activation of the lignocellulosic material may be visualized as to take place in three stages in the process of preparation: impregnation (or soaking), pyrolysis and final leaching of the impregnant. During the course of soaking, the acid introduced into the lignocellulose produces chemical changes and structural alterations, involving dehydration and redistribution of biopolymers possibly by partial dissolution in the acid solution, together with the cleavage of ether linkages between the lignin and cellulose, followed by recombination reactions in which larger structural units are formed, with the net result of a rigid crosslinked solid. Since H_3PO_4 intensely modifies the structure of the precursor, both the concentration of the impregnant and the conditions under which impregnation is carried out, must play important roles in the process [22,23]. This proposed effect is confirmed by the thermal modifications inflicted on the course of pyrolysis under the action of the acid (Fig. 1 and Table 1). Thermal decomposition is considerably shifted to higher temperatures with slow weight loss up to higher temperatures, due to the more stable macromolecular structures, indicating thus a delayed decomposition of the impregnated material in comparison to the raw precursor.

Table 6
Adsorption characteristics of MB by the various ACs

Sample	Langmuir equation		Freundlich equation		S_{MB} ($m^2 g^{-1}$)	S_{MB}/S_N^{α}
	X_m ($mg g^{-1}$)	K_L	K_F	n		
33	30.3	0.033	2.5	2.3	(73)	2.61
34	34.6	0.028	4.0	2.8	(83)	2.96
35	39.3	0.025	10.0	4.3	(94)	1.30
36	41.4	0.016	12.6	5.4	(99)	1.57
37	57.0	0.025	12.5	4.0	(168)	2.23
53	83.8	0.024	19.9	3.8	200	0.36
54	125.0	0.026	22.4	3.4	299	0.62
55	160.4	0.018	39.4	5.0	383	0.70
56	142.0	0.047	44.7	4.6	340	0.54
57	133.0	0.025	39.8	5.4	317	0.50
73	145.8	0.068	63.1	7.2	348	0.43
74	197.0	0.050	56.0	5.0	471	0.68
75	240.0	0.177	100	4.0	574	0.61
76	211.0	0.190	100	4.5	505	0.90
77	141.6	0.028	59.8	4.6	339	0.61

In the pyrolysis stage, the introduced acid dehydrates gradually with continuation of the chemical changes involving crosslinking, water elimination and polymerization. The dehydrated impregnant here reduces tar and volatiles formation, inhibits shrinkage and collapse of the particles, and develops an extensive pore structure, with a consequential increase in the carbon yield. Porosity development in this stage is ascribed to the phosphoric oxides formed at the carbonization temperatures, which act as local oxidizing agents performing controlled gasification [45]. This process actually requires the presence of very limited supply of air. It may be speculated that higher acid concentrations, or higher impregnation ratios (X_p), would enhance porosity development. However, in previous reports [24,25,30,31,53], it was demonstrated that higher acid concentrations (or X_p values) were not accompanied by a respective improvement in porosity. Rather, a loss in surface area and pore volume was noticed, which may be attributed to the formation of a layer of polyphosphate (a skin) over the developing pore structure protecting it from an excessive gasification [46]. High amounts of dehydrated, precipitated phosphorus oxides will consequently inhibit further burn-off of carbon and prevent activant attack and volatiles release, thus reducing porosity development. An acid concentration of 50–60 vol.% represents the critical value (corresponding to X_p of 1.2–1.44) in case of date pits, which is not different from previous lignocellulosic materials. Only a higher thermal treatment temperature of 700 °C, instead of 500 °C, is required to attain high and comparable surface areas (around 1000 $m^2 g^{-1}$). Still a low total pore volume is generated at this temperature (viz. 0.545 $cm^3 g^{-1}$, as compared to 0.60–1.10 $cm^3 g^{-1}$ for other precursors). This indicates the role of the precursor in determining the porosity characteristics developed under action of the H_3PO_4 activation scheme. AC obtained from date pits at 700 °C is essentially microporous which results in a high surface area product but with a low contribution of micropores to the pore volume (cf. Tables 2–4).

Finally, the third step in the preparation of AC, that is the washing and acid recovery, plays a very important role of porosity evolution. After carbonization, most of the activant is still in the particle and intense washing to eliminate it produces the porosity. It was found by Molina-Sabio et al. [7] that there is a good agreement between the volume of micropores and the volume occupied by the acid phase existing at the carbonization temperature. The entrapped polyphosphates in the final product will thus depend on its availability to

leaching, and is a function of both impregnation ratio and HTT. Both X_p and HTT are the variables of direct incidence since all carbons are post-treated under the same "standard" washing procedure. The residual entrapped dehydrated acid products will appear in the form of a high ash content (5–9%) as well as impart an acidic character on the carbon products (pH = 6.2–4.0).

5. Conclusions

Date pits are potential raw materials for producing ACs via chemical activation with H_3PO_4. These exhibit, however, two abnormal qualities: first, no detectable effect of H_3PO_4 at 300 °C and second, an extended (delayed) effect of acid at 700 °C. Low porosity carbons obtained at 300 °C show good capacity to remove substrates from solution (iodine, phenol, MB). Here, the removal seems to be associated with an absorption process by the unsaturated free bonds and radicals of the partially decomposed components irrespective of the available porosity, and the amounts taken up are many-fold higher than the N_2-surface area. ACs obtained at 500 and 700 °C are essentially microporous with some contribution of mesoporosity. The optimum activant concentration, to get the best adsorbing carbons, lies within 50 and 60 wt.% which corresponds to an acid to precursor weight ratio of 1.20–1.44. Excess acid seems to form a protective solid layer that reduces the activation of the raw material. Due to the mixed micro-/mesoporosity, the active carbons are not freely accessible to the used probe molecules from aqueous solution. The textural characteristics are the governing factor in determining the degree of uptake of these molecules. ACs obtained from date pits seem to be fairly suitable to take up contaminants from liquid effluents, and they are probably much more efficient for smaller molecules from gas streams. Activation with H_3PO_4 presents several advantages: it occurs in a single thermal treatment process, leads to a high carbon yield, the acid can be economically recovered, it is effective at relatively moderate temperatures, and it results in good adsorbents with mixed porosity that widen the scope of its application.

References

[1] B. El Duri, in: G. McKay (Ed.), Use of Adsorbents for the Removal of Pollutants from Wastewaters, Chapter 1, p. 2 and S.J. Allen, Chapter 5, p. 61, CRC Press Inc., Boca Raton, 1996.
[2] J.F. Byrne, H. Marsh, Introductory overview, in: J.W. Patrick (Ed.), Porosity in Carbons, John Wiley and Sons Inc., London, 1995.
[3] A. Bota, K. Laszlo, L.G. Nagy, T. Capitzky, Langmiur 13 (1997) 6502.
[4] R.C. Bansal, J.B. Donnet, F. Stoeckli, Active Carbon, Marcel Dekker, New York and Basel, 1988, p. 3.
[5] A.E. Pandalfo, M. Amini-Amali, J.S. Killingly, Carbon 30 (1994) 1015.
[6] J.C. Gonzalez, M.T. Gonzalez, M. Molina-Sabio, F. Rodriguez-Reinoso, A. Sepulveda-Escribano, Carbon 33 (1995) 1175.
[7] M. Molina-Sabio, F. Rodriguez-Reinoso, F. Caturla, M.J. Selles, Carbon 34 (1996) 457.
[8] K. Gergova, N. Petrov, V. Minkova, J. Chem. Tech. Biotechnol. 56 (1993) 77.
[9] F. Guzel, Sep. Sci. Technol. 10 (1993) 221.
[10] A. Bota, K. Laszlo, Per. Polytech. Ser. Chem. Eng. 41 (1997) 19.
[11] M.G. Lussier, J.C. Shull, D.J. Miller, Carbon 32 (1994) 149.
[12] K. Raveendran, A. Ganesh, K.C. Kilar, Fuel 74 (1995) 1812.
[13] R. Leboda, W. Grezerczyk, A. Lodyga, A. Dabrowski, Adsorpt. Sci. Technol. 10 (1993) 221.
[14] X. Dai, M.J. Antal Jr., Ind. Eng. Chem. Res. 38 (1999) 3386.
[15] M.S. Tam, M.J. Antal Jr., Ind. Eng. Chem. Res. 38 (1999) 268.
[16] C. Nguyen, D.D. Do, Carbon 33 (1995) 1717.
[17] A. Ahmadpour, D.D. Do, Carbon 35 (1997) 1723.
[18] R.I. Razouk, Sh. Nashed, J. Chem. UAR 8 (1965) 181.
[19] T.M. El-Akkad, Egypt. J. Chem. 21 (1978) 152,157.
[20] T.W. Ahmad, H.U. Tanzil, M. Mumtaz, Pak. J. Sci. Ind. Res. 34 (1991) 121.
[21] A.A. Attia, Adsorpt. Sci. Technol. 15 (1997) 707.
[22] F. Rodriguez-Reinoso, M. Molina-Sabio, Carbon 30 (1992) 1111.
[23] M. Molina-Sabio, F. Rodriguez-Reinoso, F. Caturla, M. Selles, Carbon 33 (1995) 1105.
[24] B.S. Girgis, L.B. Khalil, T.A.M. Tawfik, J. Chem. Tech. Biotechnol. 61 (1994) 87.
[25] C.A. Philip, B.S. Girgis, J. Chem. Tech. Biotechnol. 67 (1996) 248.
[26] L.B. Khalil, Adsorpt. Sci. Technol. 13 (1996) 317.
[27] B.S. Girgis, Bull. NRC Egypt 22 (1997) 89.
[28] A.A. El-Hendawy, S.E. Samra, B.S. Girgis, Colloids Surf. A 180 (2001) 209–221.
[29] B.S. Girgis, M.F. Ishak, Mater. Lett. 39 (1999) 107.
[30] L.B. Khalil, B.S. Girgis, T.A.M. Tawfik, Adsorpt. Sci. Technol. 18 (2000) 373.

[31] B.S. Girgis, S.S. Yunis, A.M. Soliman, J. Mater. Lett., in press.
[32] M.A. Alaya, B.S. Girgis, W.E. Mourad, J. Porous Mater. 7 (2000) 509.
[33] K.S.W. Sing, Chem. Ind. (1968) 1520.
[34] M.M. Dubinin, J. Colloid Interf. Sci. 75 (1980) 39.
[35] M.J. Selles-Perez, J.M. Martin-Martinez, J. Chem. Soc. Faraday Trans. 87 (1991) 1237.
[36] R.H. Bradley, B. Rand, J. Colloid Interf. Sci. 169 (1995) 168.
[37] V. Gomez-Serrano, C. Valenzuela-Calahorro, J. Pastor Pillegas, Biomass Bioenergy 4 (1993) 355.
[38] M. Jagtoyen, M. Thwaites, J. Stencel, B. McEnaney, F. Derbyshire, Carbon 30 (1992) 1089.
[39] M.J. Selles-Perez, J.M. Martin-Martinez, Fuel 70 (1991) 877.
[40] Tarek A.M. Tawfik, M.Sc. Thesis, Cairo University, 1994.
[41] Tarek A.M. Tawfik, Ph.D. Thesis, Cairo University, 1999.
[42] F. Carrasco-Marin, M.A. Alvarez-Merino, C. Mareno-Castilla, Fuel 75 (8) (1996) 966.
[43] M. Jagtoyen, F. Derbyshire, Carbon 36 (1998) 1085.
[44] J. Laine, S. Yunes, Carbon 30 (1992) 601.
[45] J. Laine, A. Calafat, M. Labady, Carbon 27 (1989) 191.
[46] J. Laine, A. Calafat, Carbon 29 (1991) 949.
[47] C.A. Toles, W.E. Marshall, M.M. Johns, Carbon 35 (1997) 1407.
[48] D.M. Nevskaia, A. Santianes, V. Munoz, A. Guerrero-Ruiz, Carbon 37 (1999) 1065.
[49] P.W. Collings, M. Streat, The 1996 ICHEME Event, 1996, p. 696.
[50] A.A.M. Daifullah, B.S. Girgis, Wat. Res. 32 (1998) 169.
[51] A.R. Khan, R. Atullah, A. Al-Haddad, J. Colloid Interf. Sci. 194 (1997) 154.
[52] C.H. Giles, A.P.D. D'Silva, A.S. Trivedi, Proceedings of the International Symposium on Surface Area Determination, Bristol 1969, 1970, p. 317.
[53] J.B. Castro, P.R. Bonelli, E.G. Carella, A.L. Cukierman, Ind. Eng. Chem. Res. 38 (2000) 4166.